Int. J. Heat Mass Transfer. Vol. 13, pp. 305–318. Pergamon Press 1970. Printed in Great Britain

BUBBLE DYNAMICS IN SUBCOOLED NUCLEATE BOILING BASED ON THE MASS TRANSFER MECHANISM

THEODORE T. ROBIN, JR.* and NATHAN W. SNYDER†

(*Received* 12 *February* 1969 *and in revised form* 28 *July* 1969)

Abstract—A mathematical model for bubble dynamics in subcooled nucleate boiling is derived. This model is based on the mass transfer mechanism of evaporation and condensation through the bubble. The bubble is considered to be a control volume. Heat and mass balance couples transient heat transfer caused by evaporation and condensation with bubble growth and collapse. Solutions to this model compare favorably with experimental data. This model predicts mass transfer accounts for most of the heat removed from the heated surface during subcooled nucleate boiling.

NOMENCLATURE

a, radial dimension in heated plate;
a', dimensionless a coordinate;
A_{max}, maximum value of a considered;
C_p, liquid specific heat;
C'_p, metal specific heat;
d, hydraulic diameter;
k, thermal conductivity;
$\dot{m}$, mass rate of evaporation or condensation;
M, molecular weight of fluid;
P, pressure of vapor in bubble;
P_∞, pressure of liquid in which bubble is growing;
Q, heat generation rate associated with condensation or evaporation;
r, radial coordinate;
r', dimensionless radial coordinate;
R, bubble radius;
$\dot{R}$, time derivative of R;
$\ddot{R}$, time derivative of $\dot{R}$;
R_0, universal gas constant;
t, time;
t', dimensionless time coordinate;
T, temperature;
T_d, lowest possible plate temperature (T_{sat});
T_i, initial plate temperature;
T_f, initial temperature of cooling fluid;
T_{sat}, saturation temperature corresponding to the local fluid pressure;
T_{sur}, liquid surface temperature;
$\bar{V}$, velocity vector;
y, $r' - \gamma$;
z, depth coordinate in heated plate;
z', dimensionless depth coordinate;
Z, heated plate thickness;
α, accommodation coefficient defined as the ratio of the actual amount of condensation (or evaporation) to that predicted by kinetic theory;
α_p, heated plate thermal diffusivity;
γ, dimensionless radial coordinate for bubble wall;
$\dot{\gamma}$, $d\gamma/dt'$;
ε_h, eddy thermal diffusivity in turbulent flow;
ε'_h, effective thermal diffusivity, $\dfrac{k}{\rho_l C_p} + \varepsilon_h$;
ρ, vapor density;
ρ^*, vapor saturation density at T_{sur};
ρ_1, liquid density;

* Atomics International.
† North American Rockwell Corp. Formerly Neely Professor of Nuclear and Aerospace Engineering, Georgia Institute of Technology.

ρ_p, density of heated plate;
Φ, dimensionless temperature difference in liquid;
Φ', dimensionless temperature difference in heated plate.

INTRODUCTION

SUBCOOLED nucleate boiling in forced convection is characterized by extremely high heat transfer rates. For water systems at near atmospheric pressure, heat fluxes of 10^6 Btu/h ft^2 °F and higher can be achieved [1]. Nucleate boiling heat transfer has been used in nuclear reactors and in rocket motors where economics and high performance call for high transfer rates. Full utilization of this mode of heat transfer requires reliable knowledge of its limitations—such as burnout—and full knowledge of the effect of controlable variables for performance optimization. Experimentation has been used for these purposes almost exclusively. Further, small changes in geometry, system pressure, fluid inlet conditions, etc. may require additional costly experiments. Satisfactory theoretical predictions of the complex nature of nucleate boiling in forced convection are not available. A reliable theory would be useful. Such a theory should be based on the predominant physical mechanism responsible for high heat fluxes. However, a widely accepted heat transfer mechanism for nucleate boiling does not exist.

In 1956, Snyder [2] presented the mass transfer mechanism for nucleate boiling. This mechanism is quite similar to the heat transfer process in a heat pipe. Evaporation from a hot liquid surface and subsequent condensation on a cold one results in transport of latent heat from the first surface to the second. This powerful mechanism is illustrated by heat pipes with equivalent thermal conductivities of 100 (or higher) times the thermal conductivity of solid copper, [3]. For bubbles, Snyder suggested that evaporation would occur on a thin liquid film postulated to exist on the heat surface beneath the bubble. Near the heated surface, viscous forces in the liquid inhibit its movement. During bubble growth, this thin liquid film is left on the surface. Being adjacent to the heated surface, the thin liquid film temperature is high. Evaporation on the film removes latent heat and causes a temperature decrease in the region below the bubble. Condensation occurs on the liquid surrounding the bubble top which has a lower temperature than the liquid film. This temperature difference is insured by temperature gradients resulting from the overall heat flux. Simultaneous evaporation and condensation in the bubble is the mass transfer mechanism.

Experimental evidence for the existence of the mass transfer mechanism was first observed by Moore and Messler [4]. They measured a rapid temperature decrease under a bubble in saturated pool boiling. This could be explained only by the evaporating thin liquid film. Hendricks and Sharp [5] correlated the temperature decrease with the bubble growth cycle. They observed that the decrease occurred during bubble growth rather than after bubble departure from the surface. These measurements strongly indicate an evaporating thin liquid film as required for the mass transfer mechanism. Sharp [6] has directly observed the thin liquid film by optical techniques.

Condensation on the bubble top surface has received less attention than thin liquid film evaporation. Perhaps this stems from the minimal effect of condensation for saturated pool boiling (the usual experimental condition). In this case, liquid surrounding the bubble top is at near saturation temperature. Condensation is inhibited because the temperature gradient between the thin liquid film and the bubble top surface is small. Another case of typically small temperature gradients is forced convection liquid metal heat transfer. Small temperature gradients here result from high thermal conductivity of the liquid metal and may minimize condensation. (However, in a heat pipe the mass transfer mechanism is sufficiently large to make heat conduction in solid copper negligible. Heat transfer by mass transfer through a bubble in forced convection liquid metal boiling may

be large enough to neglect heat transfer through surrounding liquid by conduction and possibly eddy diffusion.) For forced convection subcooled nucleate boiling of water at high pressures ($\sim$2000 psia), the bubble top may not grow through the thermal boundary layer because of the high pressure. Condensation may also be minimal in the case. However, for low pressure system ($<$1000 psia), the bubble is expected to grow into the subcooled turbulent stream. Condensation in this case is expected to be large. In fact, experiments have shown enormous condensation on the surface of a bubble growing in a turbulent subcooled stream [7–9]. Heat transfer coefficients of 300000 Btu/h ft^2 °F (or high) have been observed for this process.

Mass transfer is expected to be large for at least one case: Forced convection subcooled nucleate boiling of water at near atmospheric pressure. Evaporation from thin liquid films and condensation in a turbulent stream couple together giving a qualitative explanation of high heat transfer rates. A quantitative estimate of the magnitude of the mass transfer mechanism for a single bubble has been made using a mathematical model for bubble dynamics. This model considers transient conduction below the heated surface, transient evaporation, transient condensation and transient eddy diffusion in a liquid whose motion is controlled by the growing bubble.

GENERAL CONCEPTS

Items which must be considered in predicted bubble dynamics with mass transfer are:

1. Mass transfer rates between liquid and vapor phase.
2. Fluid dynamics associated with bubble growth and collapse.
3. Transient heat diffusion in the moving liquid surrounding the bubble.
4. Transient heat conduction in the heated plate.
5. Coupling the above phenomena to yield bubble dynamics.

Mass transfer across a liquid–vapor interface may be approximated from kinetic theory [10, 21]

$$\dot{m} = \alpha \left[\frac{R_0 T_{sur}}{2\pi M}\right]^{\frac{1}{2}} (\rho - \rho^*) \frac{\text{lb}}{\text{sft}^2} \qquad (1)$$

where α was assumed equal to 1·0. Fluid dynamics associated with bubble growth and collapse may be approximated with the Rayleigh equation [11]:

$$\rho_1 \{R\ddot{R} + \tfrac{3}{2}\dot{R}^2\} = P - P_\infty. \qquad (2)$$

Heat diffusion in a moving liquid may be described by:

$$\frac{\partial T}{\partial t} + \vec{V} . \nabla T = \varepsilon_h' \nabla^2 T + \frac{Q}{\rho C_p} . \qquad (3)$$

For transient heat diffusion in a solid the equation is

$$\frac{\partial T}{\partial t} = \alpha_p \nabla^2 T + \frac{Q}{\rho C_p} . \qquad (4)$$

Coupling the above items to yield bubble dynamics is accomplished with a control volume concept. Surfaces which contain the bubble vapor form the boundaries of the control volume. Rate processes represented by equations (1)–(4) are coupled by a heat and mass balance of the control volume. In this volume, vapor is assumed saturated, its temperature and pressure are assumed uniform. At any time during bubble life, the saturation density is calculated as the bubble mass divided by the bubble volume. Evaporation and condensation rates are calculated using the surface temperatures and the vapor density as required in equation (1). These rates are used to calculate the bubble mass after a small interval of time, Δt. Bubble volume (radius) at the end of Δt is calculated from equation (2). Saturation density at the end of Δt is calculated by dividing the new vapor density by the new bubble volume. Knowing the saturation density, the bubble pressure at the end of Δt is obtained from the steam tables. Surface temperature changes are calculated using equations (3) and (4) considering evaporation and condensation as surface heat sinks and sources. Changes

in the surface temperature will affect the future evaporation condensation rates [as seen in equation (1)].

Equations (1)–(3) along with the control volume concept were tested for an artificially produced vapor bubble growing in a turbulent subcooled stream [9, 12]. Mass input rate to the artificial bubble was experimentally determined. Sufficiently accurate predictions of bubble dynamics were obtained to consider these methods and assumptions valid [12].

DESCRIPTION OF BUBBLE HISTORY AND ASSUMPTIONS

Initial bubble growth is caused by bubble vapor pressure being sufficiently higher than local system pressure. Mass input to the bubble comes mainly from the evaporating thin liquid film. As latent heat is removed from the region below the bubble· the liquid film temperature decreases, causing a decrease in the mass input (evaporation) rate. Condensation represents a mass output from the bubble. As the bubble grows, the surface area of the bubble increases and causes an increase in the total mass output by condensation. Latent heat deposited at the bubble top is effectively removed by the turbulent subcooled stream. As the bubble grows, the increasing volume tends to cause a decreasing bubble pressure. Eventually, mass output exceeds mass input, and bubble pressure becomes less than the local liquid pressure. These effects and trends couple with equation (2) to yield a decreasing bubble radius: Bubble collapse.

Major assumptions for this case in addition to those previously mentioned are:

1. Initial bubble radius was assumed to be of the order of the thickness of the buffer layer as calculated from the general velocity distribution using the stream velocity and hydraulic diameter.

2. Initial temperature distribution in the heated plate was assumed uniform. (And equal to the value estimated by Bankoff [13]).

3. Initial temperature of the liquid was assumed equal to the center line temperature except for a thin shell of liquid surrounding the bubble, the temperature of which was assumed equal to the plate temperature.

4. Initial state of the vapor in the bubble was assumed to be saturation corresponding to the plate temperature.

5. Relative velocity between bubble and heated plate was assumed zero. Relative velocity between stream and bubble surface was assumed zero. Liquid motion occurred only in the r direction, and liquid temperature distribution was a function of r and t only. Coordinate system for this problem is shown in Fig. 1.

6. Heat generation rate in the plate was assumed uniform, and the opposite side of the plate was insulated.

7. ε_h' was assumed to be independent of time and position.

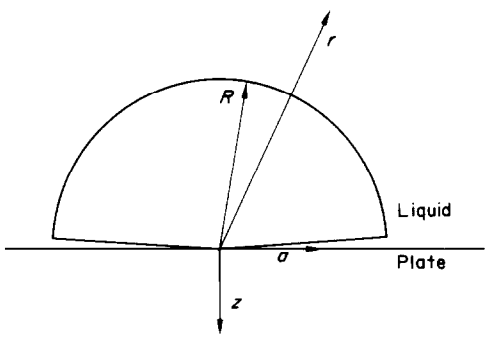

FIG. 1. Variable for a bubble in subcooled nucleate boiling.

The assumption concerning initial bubble radius was based on the nature of the initial period of bubble growth. This growth is rapid and vapor is supplied from all of the bubbles surface by superheated liquid in the buffer layer. From this point the mechanism departs to the mass transfer model as the bubble grows out into the subcooled region. Almost all of the heat transfer occurs at a bubble radius about 20 times the assumed initial size.

Assumption 5 neglects the motion of the

bubble along the heated plate. The amount of movement, however, is only about $\frac{1}{2}$ the maximum bubble diameter for a velocity of 10 ft/s. Further, Fig. 7 indicates that once a portion of the plate surface has been exposed to the bubble vapor, the temperature of the freshly exposed surface quickly drops so that the temperature of the entire exposed surface is approximately the same value. Thus, the heat removal rate from the plate would depend more on the exposed area of the thin liquid film than its position along the plate.

HEAT DIFFUSION FROM BUBBLE SURFACE

Liquid velocity as a function of radius may be represented as $R^2\dot{R}/r^2$ [11]. Equation (3) may be written as

$$\frac{\partial T}{\partial t} + \frac{R^2\dot{R}}{r^2}\frac{\partial T}{\partial r} = \varepsilon_h'\left(\frac{\partial^2 T}{\partial r^2} + \frac{2}{r}\frac{\partial T}{\partial r}\right) + \frac{Q}{\rho_l C_p} \quad (5)$$

where Q represents the heat of condensation at the bubble surface. Now let

$$r' = \frac{2r}{\mathrm{d}}$$

$$\gamma = \frac{2R}{d}$$

$$t' = \frac{4\varepsilon_h'}{d^2}t$$

and

$$\Phi = \frac{T - T_f}{T_{\mathrm{sat}} - T_f}.$$

Using the above definitions, equation (5) becomes:

$$\frac{\partial \Phi}{\partial t'} + \frac{\gamma^2}{r'^2}\dot{\gamma}\frac{\partial \Phi}{\partial r'} = \frac{\partial^2 \Phi}{\partial r'^2} + \frac{2}{r'}\frac{\partial \Phi}{\partial r'} + \frac{Q(d)^2}{4\varepsilon_h'\rho_l C_p(T_{\mathrm{sat}} - T_f)}. \quad (6)$$

Also, with the transformation $y = r' - \gamma$, equation (6) becomes:

$$\frac{\partial \Phi}{\partial t'} - \dot{\gamma}\left[1 - \frac{1}{(1 + y/\gamma)^2}\right]\frac{\partial \Phi}{\partial y} = \frac{\partial^2 \Phi}{\partial y^2} + \frac{2}{\gamma(1 + y/\gamma)}\frac{\partial \Phi}{\partial y} + \frac{Q(d)^2}{4\varepsilon_h'\rho_l C_p(T_{\mathrm{sat}} - T_f)}. \quad (7)$$

The boundary conditions are $\partial\Phi/\partial y = 0$ for $y = 0$ and $y_{\max}$ which is a substantial distance from the bubble radius.

Numerical approximation for this equation is developed in [9].

HEAT DIFFUSION IN HEATED PLATE

A cylindrical coordinate system was chosen for the heated plate for which $T = T(a, z, t)$ (see Fig. 1). The z axis passes through the center of the bubble. For this case, the heat diffusion equation is:

$$\frac{\partial T}{\partial t} = \alpha_p\left(\frac{\partial^2 T}{\partial a^2} + \frac{1}{a}\frac{\partial T}{\partial a} + \frac{\partial^2 T}{\partial z^2}\right) + \frac{Q}{\rho_p C_p'} \quad (8)$$

where Q is heat generation rate in plate and a surface sink caused by evaporation. Since this equation was solved simultaneously with (7), the same time scale was used here. This is $t' = 4t\varepsilon_h'/(d)^2$. Also, the following definitions were made:

$$\Phi' = \frac{T - T_i}{T_d - T_i}$$

$$z' = z/Z$$

$$a' = a/A_{\max}.$$

With the above definitions, equation (8) becomes:

$$\frac{\partial \Phi'}{\partial t'} = \frac{\alpha_p}{4\varepsilon_h'}\frac{(d)^2}{(A_{\max})^2}\left(\frac{\partial^2 \Phi'}{\partial a'^2} + \frac{1}{a'}\frac{\partial \Phi'}{\partial a'}\right) + \frac{\alpha_p}{4\varepsilon_h'}\frac{(d)^2}{z'^2}\frac{\partial^2 \Phi'}{\partial z'^2} + \frac{Q(d)^2}{4\varepsilon_h'\rho_p C_p'(T_d - T_i)} \quad (9)$$

The boundary conditions are $\partial\Phi/\partial a' = 0$ for $a' = 0$ and 1, $\partial\Phi'/\partial z' = 0$ for $z' = 0$ and 1, which corresponds to a substantial distance from the bubble radius. The numerical approximation to this equation is developed in [9].

METHOD OF ADVANCING THE NUMERICAL SOLUTION

After the solution had been advanced up to a time, t, the following quantities were known:

1. State of the steam in the bubble (density and pressure).
2. R, $\dot{R}$, $\ddot{R}$ and the bubble volume.
3. Amount of mass in the bubble.
4. Liquid temperature at the surface of the bubble.
5. Temperature of the thin liquid film.
6. Temperature of the surface of the heated plate.
7. Temperature distributions in both the liquid and the heated plate.
8. Amount of liquid in the thin liquid film.

To advance the solution an increment of time, the following procedure was used:

1. Since R, $\dot{R}$, $\ddot{R}$ and the bubble vapor pressure were known, the changes in R, $\dot{R}$ and $\ddot{R}$ were calculated with the aid of equation (2), a three term Taylor series expansion for R, and a two term Taylor series expansion for $\dot{R}$.
2. Using equation (1), the amount of vapor condensed was calculated by first finding the saturation vapor density corresponding to the known liquid surface temperature. This value and the known bubble vapor density were then used in equation (1) and the amount of condensation calculated.
3. Amount of liquid which would evaporate from the thin liquid film during the time increment was calculated next. First, the saturation vapor corresponding to the temperature of the thin liquid film was obtained. Then the evaporation rate was calculated, and from this the amount which evaporated was obtained.
4. Total mass in the bubble at the end of the time interval was calculated by adding to the old total mass the difference between the mass evaporated and the mass condensed.
5. New bubble volume was calculated using the results of step 1. This volume was divided into the new mass found in step 3, and the result was the new density. Since the vapor in the bubble was assumed saturated, the new pressure was obtained from the steam tables.
6. Latent heat represented by condensed steam was then used along with the numerical approximation to equation (7) to calculate new liquid surface temperature and new temperature distribution in the liquid.
7. Latent heat represented by evaporated liquid from the thin liquid film together with the numerical approximation to equation (9) was used to calculate the new plate surface temperature and the new temperature distribution in the heated plate.
8. Finally, the amount of mass evaporated was subtracted from the total mass in the thin liquid film to give the new total mass in the film.

RESULTS AND DISCUSSION

Most of the parameters in the above equations are known with reasonable accuracy. ε'_h in equation (3), however, is not. For single phase flow ε'_h may be predicted with good accuracy. For boiling, growth and collapse of bubbles near the heated surface are expected to modify this value. In using the theoretical model, several values of ε'_h were assumed. Through a comparison of theoretical predictions with experimental results, a proper value of ε'_h could be determined within the limits of the assumptions made in developing the mathematical model. Experimental results used for this comparison were bubble radius vs. time curves. Gunther reported several radius vs. time curves for subcooled nucleate boiling in forced convection. Water was the fluid, and stainless steel was assumed for the heated plate. Experimental conditions used for the comparison between theory and experiment were (see [1], p. 119, Fig. 9): heat flux, 2·75 Btu/in^2 s; fluid velocity, 10 ft/s; pressure, 28·8 in Hg; and subcooling, 90°F (bulk liquid temperature, 122°F). Bankoff [13] estimated the wall temperature to be 287°F. Several experimental curves for these conditions are reproduced in Fig. 2.

Several preliminary runs were made with an initial liquid temperature of 110°F. Bubble radius vs. time curves for these cases are shown in Fig. 3. Except for curve number 2, initial thin liquid film thickness was assumed larger

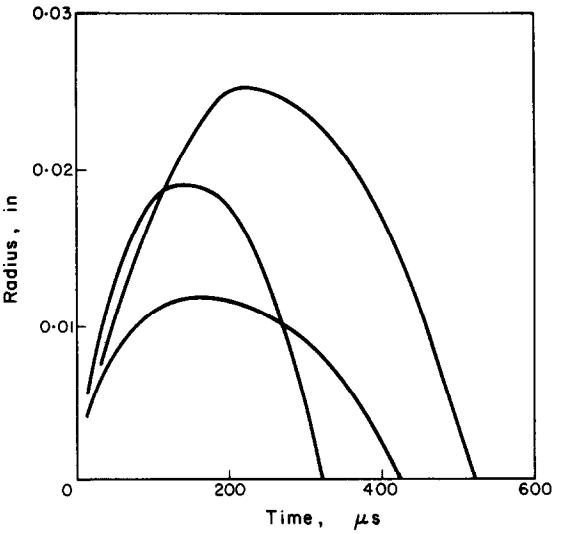

FIG. 2. Experimental bubble radius as a function of time for subcooled nucleate boiling in forced convection: $q/A = 2{\cdot}75$ Btu/in^{2}s; $V = 10$ ft/s; $P = 28{\cdot}8$ in Hg; $\Delta T_{sub} = 90°F$ (Gunther, [1]).

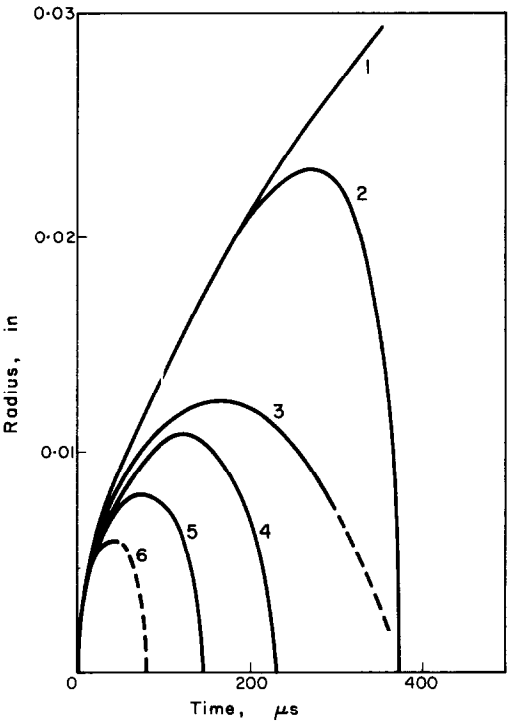

FIG. 3. Bubble radius as a function of time for the real boiling model: $P_\infty = 14{\cdot}2$ psia; $T_L = 110°F$; initial plate temperature = 287°F; heat generation rate = $4{\cdot}3 \times 10^9$ Btu/h ft^3;

(1) $\varepsilon_h' = 0{\cdot}07$ ft^2/h, $\delta_{min} = 1{\cdot}72 \times 10^{-4}$ ft.
(2) $\varepsilon_h' = 0{\cdot}07$, $\delta_{min} = 1{\cdot}1 \times 10^{-5}$
(3) $\varepsilon_h' = 0{\cdot}082$, $\delta_{min} = 1{\cdot}0 \times 10^{-5}$
(4) $\varepsilon_h' = 0{\cdot}085$, $\delta_{min} = 1{\cdot}4 \times 10^{-5}$
(5) $\varepsilon_h' = 0{\cdot}095$, $\delta_{min} = 1{\cdot}12 \times 10^{-5}$
(6) $\varepsilon_h' = 0{\cdot}12$, $\delta_{min} = 6{\cdot}6 \times 10^{-6}$.

than required. That is, thin liquid film "dry up" was not allowed. Reported in Fig. 3, δ_{min} is the minimum film thickness required to produce the corresponding curve. Any δ larger than δ_{min} would produce the same curve for the present model which neglects thermal resistance of the thin film. For curve number 2, the initial thickness was fixed at $1{\cdot}1 \times 10^{-5}$ ft and at approximately 150 μs, this film had dried up near the centre of the bubble. As growth continued beyond this point, thin liquid film dry up proceeded. Mass input rate decreased rapidly, initiating bubble collapse. However, the shape of this curve does not compare well with those observed experimentally by Gunther [1]. This result seems to indicate that complete thin liquid film dry up does not occur in this region of boiling. This implies that thin liquid film supply exceeds the demand. One possible source of fluid for the thin liquid film may be the liquid adjacent to the wall just downstream of the bubble. Since Gunther's bubbles move over the plate with a velocity 0·8 times the stream velocity, they are continually exposed to a fresh supply of thin liquid film.

In Gunther's case the actual liquid temperature was approximately 122°F. Results of a few cases using the complete physical data for Gunther's case are shown in Fig. 4. Curves 1–3 differ only in the choice of ε_h', and it is observed that the maximum bubble radius is a strong function of ε_h'. Curve 5 has the same value of ε_h' as curve 3; however, the cooling liquid temperature has been lowered 4°F. This indicates a strong dependence of the maximum bubble radius on the local liquid temperature. Values for the maximum bubble radius observed by Gunther varies from a low of approximately 0·012 in. to a high of approximately 0·026 in. (see Fig. 2).

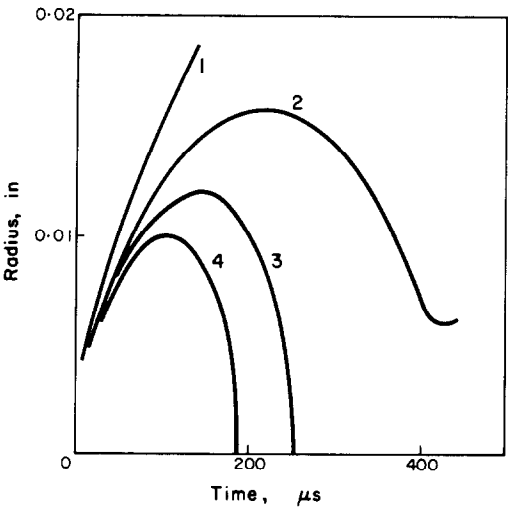

FIG. 4. Bubble radius as a function of time for the real boiling model for conditions as in Gunther's experiment (see Fig. 2):
(1) $\varepsilon_h' = 0{\cdot}087$ ft^2/h, $\delta_{min} = 1{\cdot}43 \times 10^{-5}$ ft, $T_L = 122$°F
(2) $\varepsilon_h' = 0{\cdot}105$, $\delta_{min} = 2{\cdot}0 \times 10^{-5}$, $T_L = 122$
(3) $\varepsilon_h' = 0{\cdot}11$, $\delta_{min} = 1{\cdot}48 \times 10^{-5}$, $T_L = 122$
(4) $\varepsilon_h' = 0{\cdot}105$, $\delta_{min} = 1{\cdot}28 \times 10^{-5}$, $T_L = 118$.

A partial explanation for the large range of values for the maximum radius appears to be small variations in the local value of ε_h' and in the local temperature which are present in a turbulent stream. Curves 4 and 5 are reasonably similar to those observed by Gunther. Curve 3 is also similar except the bubbles observed by Gunther completely collapsed. Curve 3 would have gone to zero radius if some thin liquid film dry out had occurred. This possibility definitely exists.

Comparison of Figs. 2 and 4 shows that accurate bubble dynamics can be predicted with a model based on mass transfer. However, several assumptions were required. ε_h' and thin liquid film thickness are important ones.

ε_h' was assumed to be about 0·1 ft^2/h to produce the curves in Fig. 4. ε_h' should be about 1·0 ft^2/h as estimated from fully developed pipe flow turbulence theory. One possible cause of this disagreement is the assumed value of the initial liquid temperature near the bubble. This was asssumed to be the bulk fluid temperature considering the low thermal resistance of the turbulent core. However, Jiji and Clark [14] demonstrated that the liquid temperature near the bubbles may be much higher than the bulk temperature. A higher value for the initial liquid temperature would tend to reduce the rate of mass output by condensation. A corresponding higher value of ε_h' would be required to counteract this trend and yield the same radius vs. time.

Alternately, a low value of ε_h' may be justified. Tong [15] has commented on recent results of Adorni *et al.* [16]:

> "... Consider next the turbulent flow in which the momentum exchanged is accomplished by turbulent velocity eddies. The presence of drops or bubbles will reduce the turbulent mixing or momentum exchange between adjacent fluid layers for two reasons. First, the dispersed discontinuous phase hinders the free path of turbulent eddies by intermittently separating adjacent layers of the continuous phase. Second, part of the momentum of the eddies meant for exchange is absorbed in the displacement and deformation of the discontinuous phase. The resulting suppression of momentum exchange in the turbulent core is mathematically manifested in terms of a reduced mixing length constant. Physically, it shows up in a shape of velocity profiles less flat than for turbulent flow of either of the phases alone. This interpretation of profile shapes in terms of increased apparent viscosity and suppressed turbulence due to the presence of discontinuous phase applies equally well to both bubbly and droplet flows."

If these comments may be applied to the bubble region in subcooled nucleate boiling, eddy thermal diffusivity may be lower than expected because of the reduced mixing length. This implication is in drastic conflict with the bubble agitation explanation of nucleate boiling. However, it does support the low value of ε_h' required in the solution to the model.

Values for the initial thin liquid film thickness in subcooled nucleate boiling in forced convection have not been experimentally measured. However, several values have been reported for pool boiling. Moore and Messler [4] reported values between 80 and 90 μin. Hospeti and Mesler [17] reported values between 20 and 100 μin. Cooper and Lloyd [18] reported values between 100 and 800 μin. Sharp [6] reported a value of about 15 μin. Values required to produce accurate radius vs. time curves reported here were between 100 and 180 μin. This agreement is good and represents another point of confidence for this model.

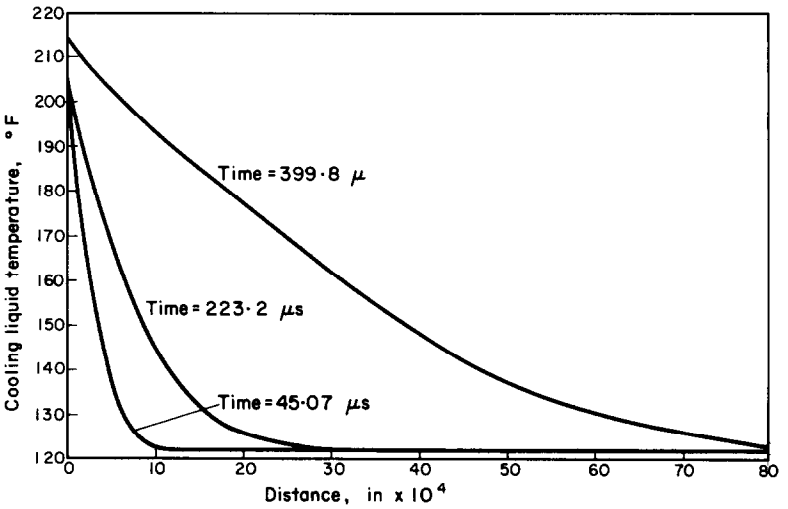

FIG. 5. Cooling liquid temperature as a function of radial distance from the bubble surface for the real boiling model for conditions as in Gunther's experiment.

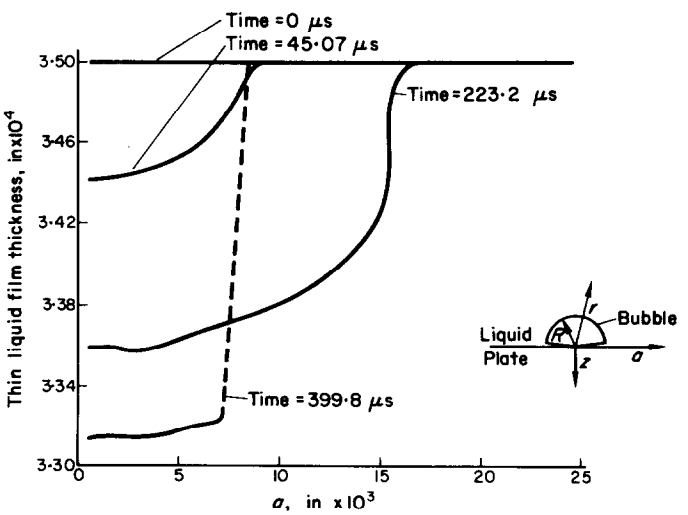

FIG. 6. Thin liquid film thickness as a function of a for the real boiling model for conditions as in Gunther's experiment.

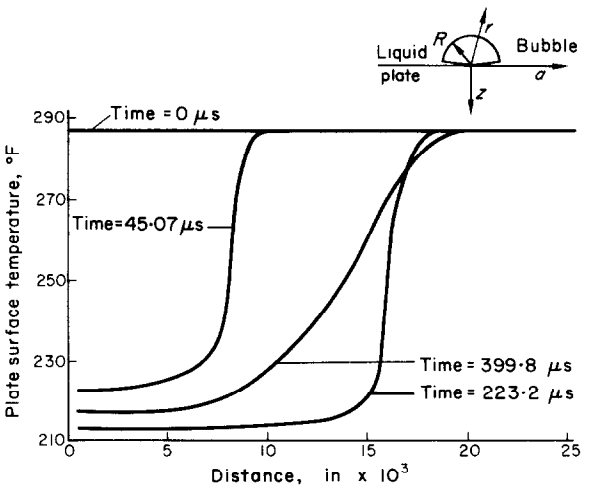

FIG. 7. Plate surface temperature as a function of a for the real boiling model for conditions as in Gunther's experiment.

A major objective in the development and solution of this model was to estimate the importance of the mass transfer mechanism. Rohsenow and Clark [19] concluded that bubble agitation was responsible for high heat transfer rates in boiling and latent heat effects were negligibly small. However, they neglected simultaneous vaporization and condensation.

For the boiling case studied here, Gunther [1] reported about 760 000 bubbles/in^2 s and a heat flux of 2·75 Btu/in^{2}s. Assuming that all heat transferred from the plate was associated with mass transfer through the bubbles only, the total heat removed by one bubble would be

$$\frac{2{\cdot}75\ \text{Btu/in}^2\ \text{s}}{760\,000\ \text{bubbles/in}^2\ \text{s}} = 3{\cdot}62 \times 10^{-6}\ \frac{\text{Btu}}{\text{bubble}}$$

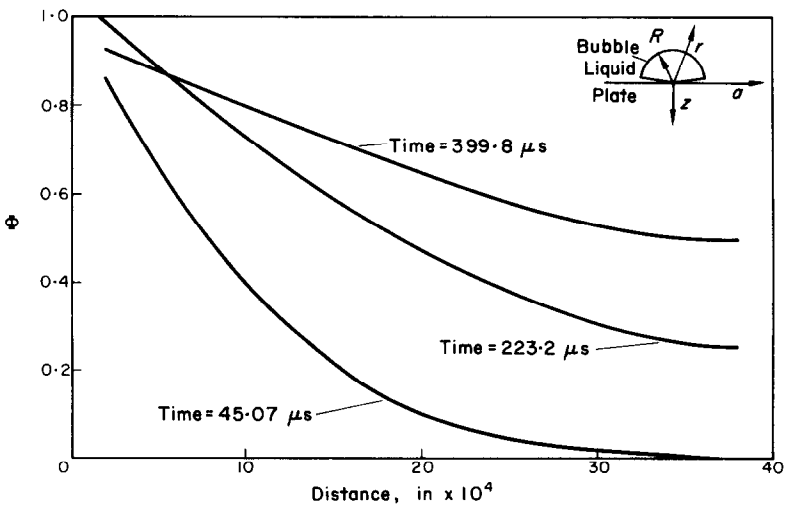

FIG. 8. Dimensionless temperature difference in heated plate for $a = 0$ as a function of z for the real boiling model for conditions as in Gunther's experiment.

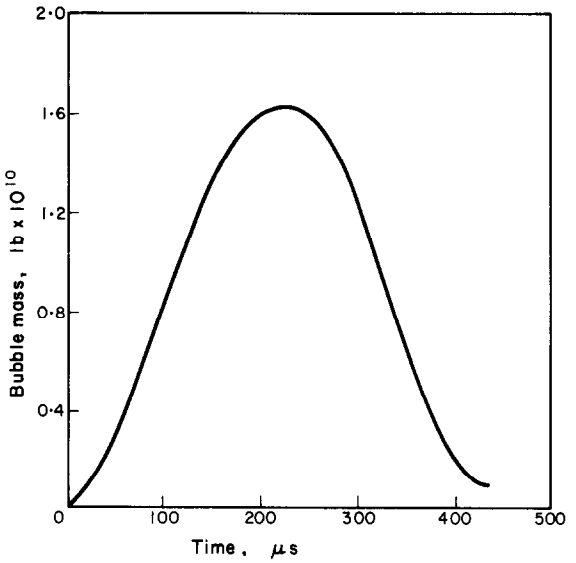

FIG. 9. Bubble mass as a function of time for the real boiling model for conditions as in Gunther's experiment.

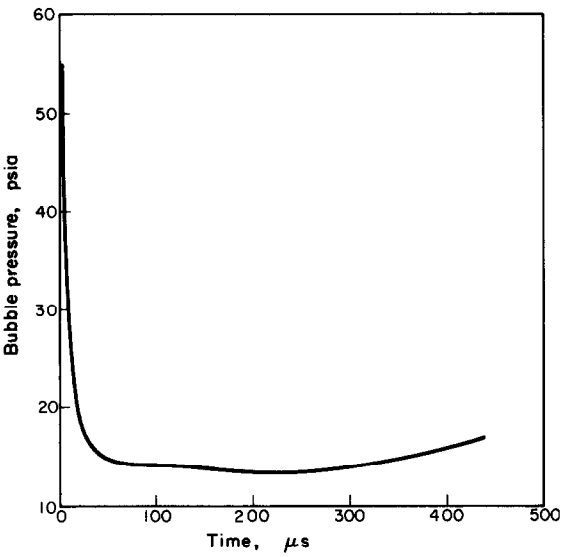

FIG. 10. Bubble pressure as a function of time for the real boiling model for conditions as in Gunther's experiment.

For curve number 2 of Fig. 4, the total amount of heat was $5{\cdot}17 \times 10^{-6}$ Btu.

Figs. 5–15 are presented in order to further characterize this model. These correspond to curve number 2 of Fig. 4. The initial plate temperature was assumed 287°F. Figs. 5–8 represent the following at various times during the bubble life: (a) liquid temperature as a function of distance from the surface of the bubble; (b) thin liquid film thickness as a function of a, the radial distance on the plate surface; (c)

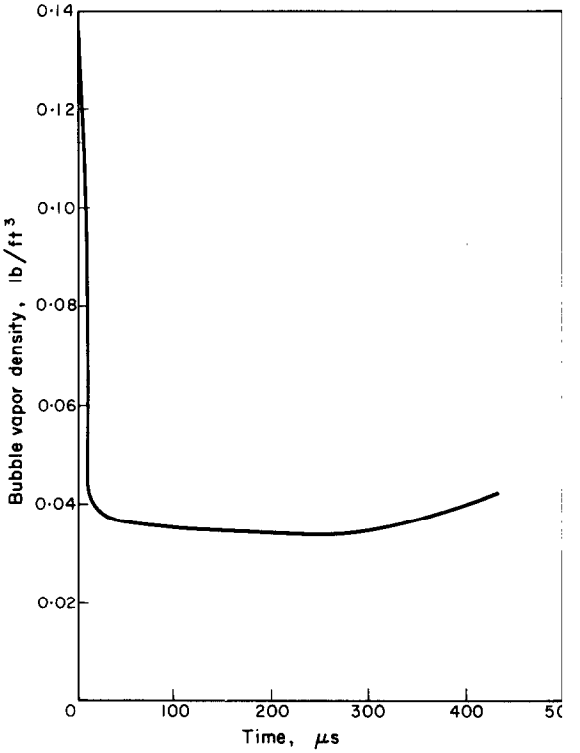

FIG. 11. Bubble vapor density as a function of time for the real boiling model for conditions as in Gunther's experiment.

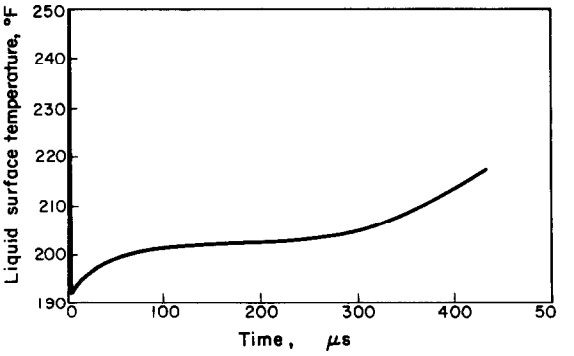

FIG. 12. Liquid surface temperature as a function of time for the real boiling model for conditions as in Gunther's experiment.

plate surface temperature as a function of a; (d) dimensionless temperature in heated plate as a function of distance into the plate, z, for $a = 0$. Figs. 9–14 represent the bubble mass, the bubble pressure, the density of the vapor in the bubble, the cooling liquid surface temperature, the heated plate surface temperature for $a = 0$, the thin liquid film thickness for $a = 0$, respectively, as they vary with time. Figure 15 shows the total amount of heat removed from the plate per unit of time and the heat flux through the bubble base as functions of time.

It is interesting to note that the bubble vapor pressure is about system pressure during most of the bubble life. Also, most of the heat removal from the plate occurs when the bubble is large.

It is hoped that theoretical and experimental investigations of the mass transfer mechanism will lead to a basic understanding of the mechanism of heat transfer in subcooled nucleate boiling. This research is leading to a basic theory which the authors have been developing to describe the q/A vs. ΔT boiling curve as well as

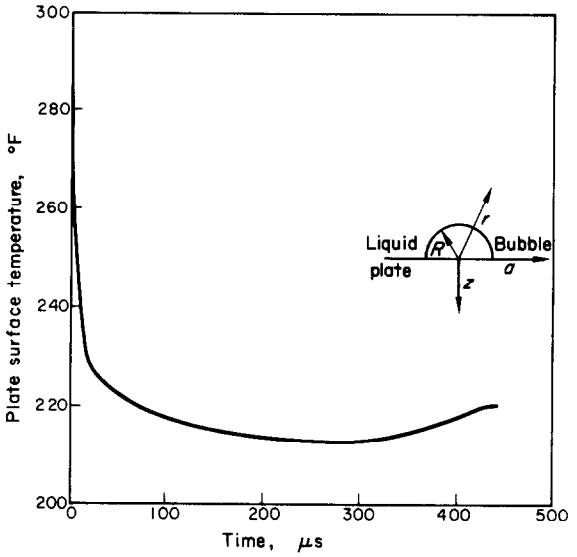

FIG. 13. Plate surface temperature for $a = 0$ as a function of time for the real boiling model for conditions as in Gunther's experiment.

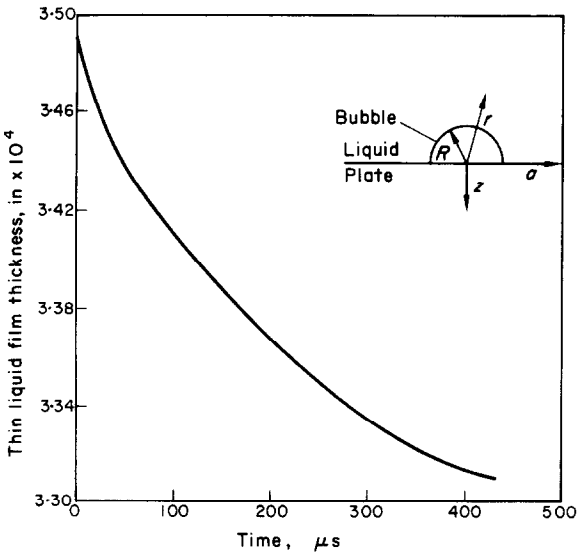

FIG. 14. Thin liquid film thickness for $a = 0$ as a function of time for the real boiling model for conditions as in Gunther's experiment.

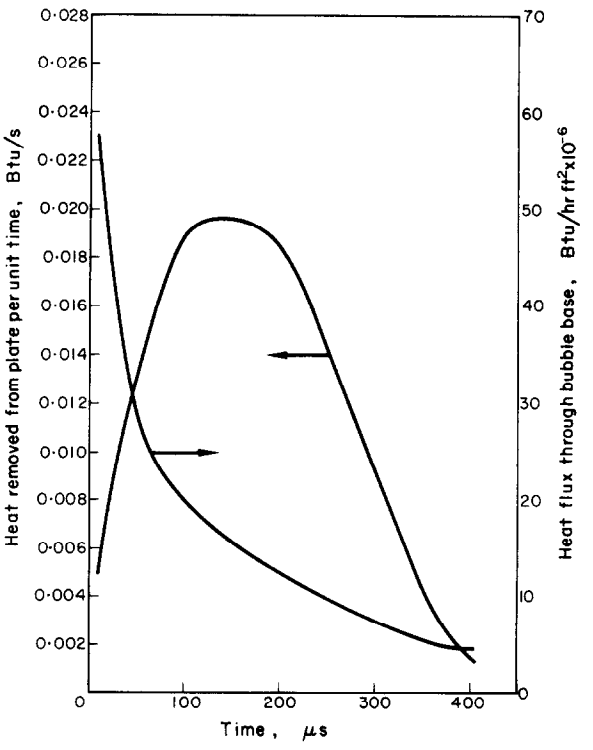

FIG. 15. Heat removed from plate per unit of time and heat flux through bubble base as functions of time for the real boiling model for conditions as in Gunther's experiment.

the mechanism at the peak (burnout point). It will lead to design equations for boiling heat transfer which are more in keeping with the physical mechanisms.

CONCLUSIONS

1. Mass transfer mechanism is important and may account for almost all of the heat transfer in subcooled nucleate boiling.

2. Bubble dynamics in subcooled boiling can be predicted with a mathematical model based on the mass transfer mechanism.

REFERENCES

1. F. C. GUNTHER, Photographic study of surface-boiling heat transfer to water with forced convection, *Trans. Am. Soc. Mech. Engrs* **73**(2), 115–124 (1951).
2. N. W. SNYDER, Comments on pp. 13, 14, 15, 20, 21, 38 and 39 of [20].
3. G. M. GROVER, T. P. COTTER and G. F. ERICKSON, Structures of very high thermal conductance, *J. Appl. Phys.* 1990, June (1964).
4. F. D. MOORE and R. B. MESLER, The measurement of rapid surface temperature fluctuations during nucleate boiling of water, *A.I.Ch.E. Jl* **7**(4), 620 (1961).
5. R. C. HENDRICKS and R. R. SHARP, Initiation of cooling due to bubble growth on a heating surface, NASA TN *D*-2290, Lewis Research Center (1964).
6. R. R. SHARP, The nature of liquid film evaporation during nucleate boiling, NASA TN *D*-1997, Lewis Research Center (1964).
7. S. G. BANKOFF and J. P. MASON, Heat transfer from the Surface of a steam bubble in turbulent subcooled liquid stream, *A.I.Ch.E. Jl* **8**(1), 30 (1962).
8. N. W. SNYDER and T. T. ROBIN, Mass transfer model in subcooled nucleate boiling, *J. Heat Transfer* 404–412, August (1969).
9. T. T. ROBIN, Mass transfer effects in subcooled nucleate boiling, Ph.D.Thesis, Georgia Institute of Technology, Atlanta, Ga. November (1966).
10. E. H. KENNARD, *Kinetic Theory of Gases*. McGraw-Hill, New York (1938).
11. H. LAMB, *Hydrodynamics* 6th edn., p. 122. Cambridge (1932).
12. T. T. ROBIN and N. W. SNYDER, Theoretical analysis of bubble dynamics for an artificially produced vapor bubble in a turbulent stream, submitted for publication, *Int. J. Heat and Mass Transfer*.
13. S. G. BANKOFF, On the mechanism of subcooled nucleate boiling, Jet Propulsion Laboratory Memo 30–38 (1959).
14. L. M. JIJI and J. A. CLARK, Bubble boundary layer and temperature profiles for forced convection boiling in channel flow, *J. Heat Transfer* 50–58, February (1964).
15. L. S. TONG, *Boiling Heat Transfer and Two-Phase Flow*, p. 72. John Wiley, New York (1965).
16. N. ADORNI *et al.*, An isokinetic sampling probe for phase and velocity distribution measurements in two-phase flow near the wall of the conduit, *CISE Report* R-89, Milan (1963).
17. N. B. HOSPETI and R. B. MESLER, Deposits formed beneath bubbles during nucleate boiling of radioactive calcium sulfate solutions, *A.I.Ch.E. Jl* **11**(4), 662 (1965).
18. M. G. COOPER and A. J. P. LLOYD, Transient local heat flux in nucleate boiling, 3*rd Int. Heat Transfer Conf.*, Chicago (1966).
19. W. M. ROHSENOW and J. A. CLARK, A study of the mechanism of boiling heat transfer, *Trans. Am. Soc. Mech. Engrs* **73**(5), 609–620 (1951).
20. S. G. BANKOFF, W. J. COLAHAN, JR. and D. R. BARTZ, Summary of conference on bubble dynamics and boiling heat transfer held at the Jet Propulsion Laboratory, Jet Propulsion Laboratory Memo., 20–137, June 14 and 15 (1956).
21. J. B. TAYLOR and I. LANGMUIR, The evaporation of atoms, ions and electrons from caesium films on tungsten, *Phys. Rev.*, **44**(6), 444, September (1933).

DYNAMIQUE DES BULLES DANS L'EBULLITION NUCLEEE SOUS-REFROIDIE BASEE SUR LE MECANISME DU TRANSPORT DE MASSE

Résumé—Un modèle mathématique est obtenu pour la dynamique des bulles dans l'ébullition nucléée sous-refroide. Ce modèle est basé sur le mécanisme de transport de masse de l'évaporation et de la condensation à travers la bulle. On considère la bulle comme un volume de contrôle. Le bilan de chaleur et de masse couple le transport de chaleur transitoire provoqué par l'évaporation et la condensation avec la croissance et la disparition des bulles. Les solutions de ce modèle se comparent favorablement avec les résultats expérimentaux. Ce modèle prédit que le transport de masse rend compte de la plus grande partie de la chaleur enlevée de la surface chauffée l'ébullition nucléée sous-refroidie.

BLASENDYNAMIK BEI UNTERKÜHLTEM SIEDEN AUF GRUND DES STOFF TRANSPORTMECHANISMUS

Zusammenfassung—Es wird ein mathematisches Modell für die Blasendynamik bei unterkühltem Sieden abgeleitet. Dieses Modell basiert auf dem Stofftransportmechanismus beim Verdampfen und Kondensieren

in der Blase. Die Blase wird als ein Regelvolumen betrachtet. Wärme- und Stoffbilanz verbinden den instationären Wärmeübergang, der sich beim Verdampfen und Kondensieren, beim Blasenwachstum und Zusammenfallen ergibt. Lösungen für dieses Modell stimmen gut mit experimentellen Werten überein. Das Modell besagt, dass der Stofftransport verantwortlich ist für den grössten Wärmeanteil, der von der Heizfläche bei unterkühltem Blasensieden abgeführt wird.

ДИНАМИКА РОСТА ПУЗЫРЬКА ПРИ ПУЗЫРЬКОВОМ КИПЕНИИ НЕДОГРЕТОЙ ЖИДКОСТИ НА ОСНОВАНИИ МЕХАНИЗМА ПЕРЕНОСА МАССЫ

Аннотация—Выведена математическая модель динамики роста пузырька при пузырьковом кипении переохлажденной жидкости. Эта модель основана на механизме массопереноса при испарении и конденсации. Пузырек считается контрольным объемом. Баланс тепла и массы связывает неустановившийся перенос тепла при испарении и конденсации с ростом и разрушением пузырьков. Результаты теоретических расчетов хорошо подтверждаются экспериментальными данными. С помощью этой модели рассчитывается поток массы за счет большей части тепла, уносимого с поверхности во время пузырькового кипения переохлажденной жидкости.